Supplement of Weather Clim. Dynam., 7, 1133–1152, 2026
https://doi.org/10.5194/wcd-7-1133-2026-supplement

Supplement of

Revisiting the surface impacts of the QBO in the Large Ensemble Single Forcing MIP simulations: are teleconnections still too weak?

Chaim I. Garfinkel et al.

Correspondence to: Chaim I. Garfinkel (chaim.garfinkel@mail.huji.ac.il)

S1 Contents of this file

1. Figures S1 to S13

S2 Introduction

In the Supporting Information, we show details which are not shown in the main manuscript. Figure S1-S4 document the QBO in snapshots from each of the four models. Figure S5-S7 assess sensitivity to using a compositing approach instead of a regression approach to quantify zonal mean teleconnections. Figures S8-S9 assess sensitivity to defining the QBO with 30hPa winds rather than 50hPa winds. Figure S10 shows the surface response to the QBO using ERA5 data. Figure S11 assesses sensitivity to regressing out the linear influence of ENSO before considering QBO impacts on U700, and also shows U700 teleconnections since 1970 only. Figure S12 considers the surface temperature response to the QBO since 1970. Figure S13 shows that the QBO's MMC strengthens as GHG increase, which leads to stronger teleconnections in some regions.

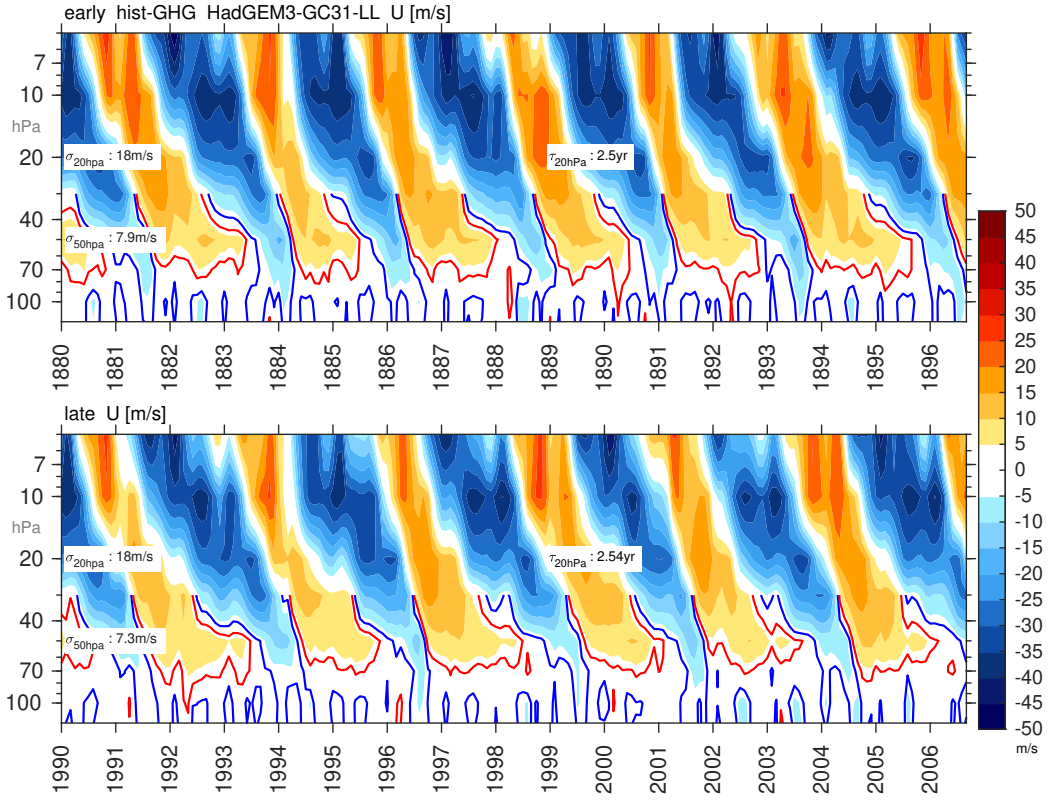

Figure S1. Zonal mean zonal wind from 5S-5N in hist-GHG for 1880-1997 and 1990-2007 for the first ensemble member of HadGEM3. Each panel also indicates the periodicity of the 20hpa winds, and also the standard deviation of the QBO winds at 20hPa and 50hpa, averaged over all ensemble members and computed over the (a) 1850-1931 and (b) 1932-1979. The $\pm$ 2.5m/s isotach is included in blue and red below 30hPa.

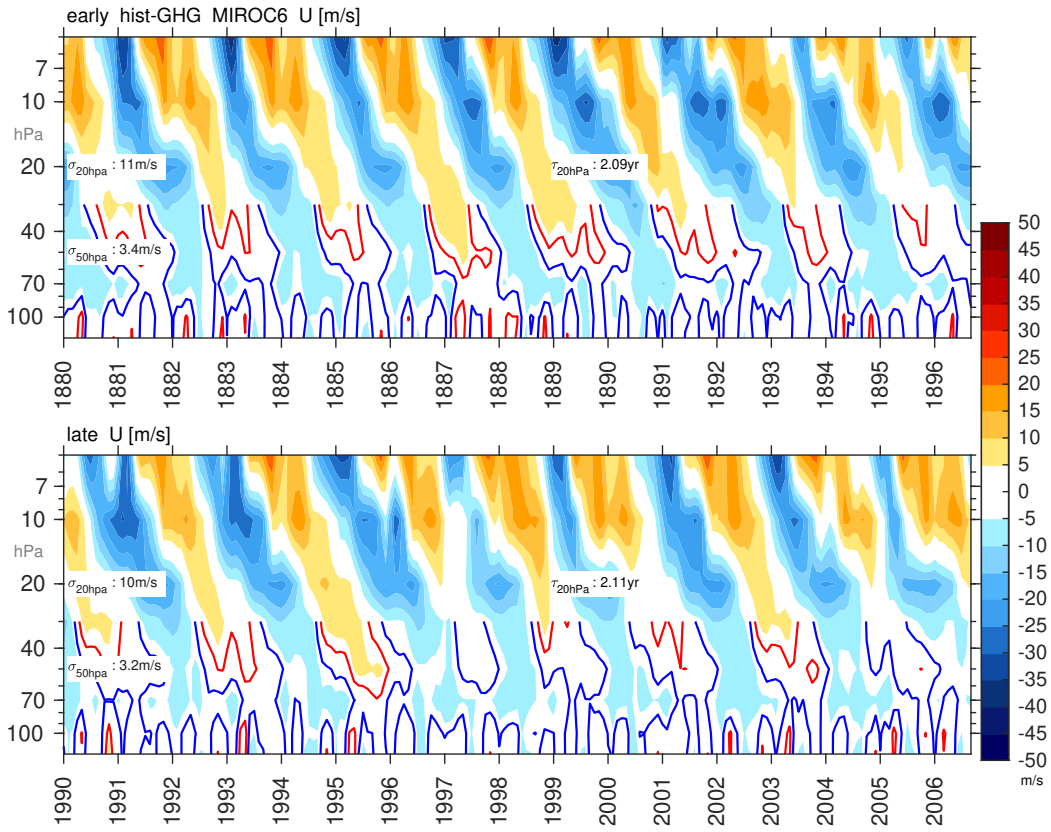

Figure S2. As in Figure S1 but for MIROC6.

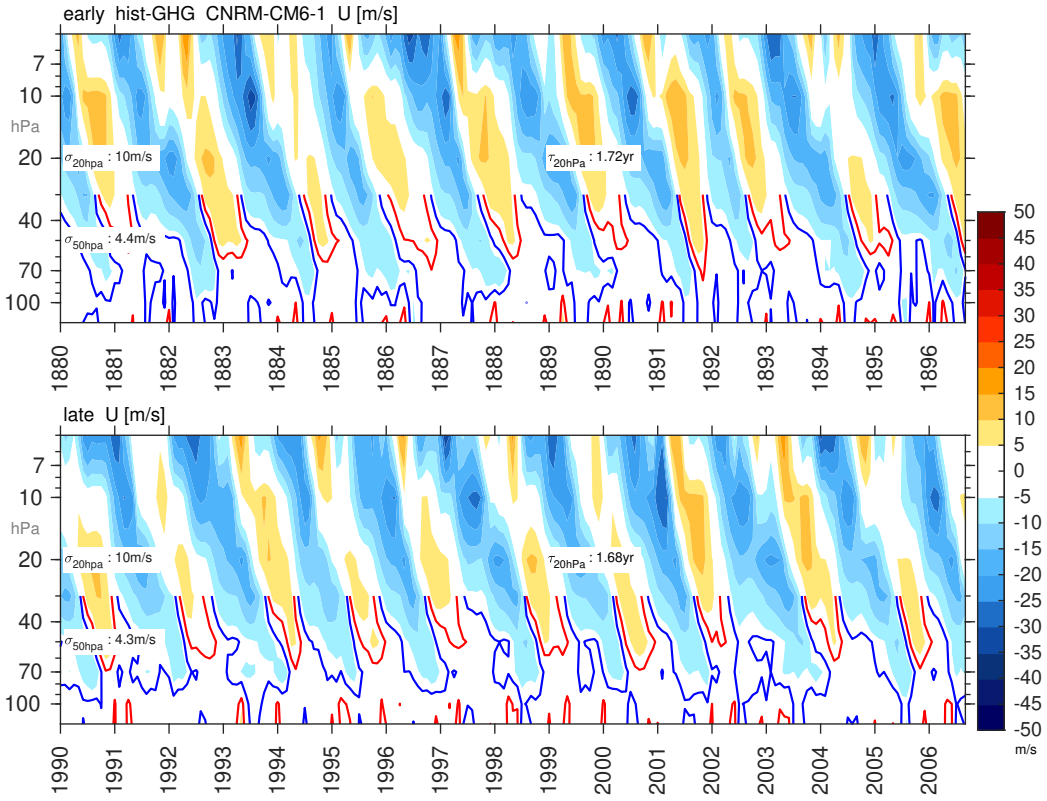

Figure S3. As in Figure S1 but for CNRM-CM6-1.

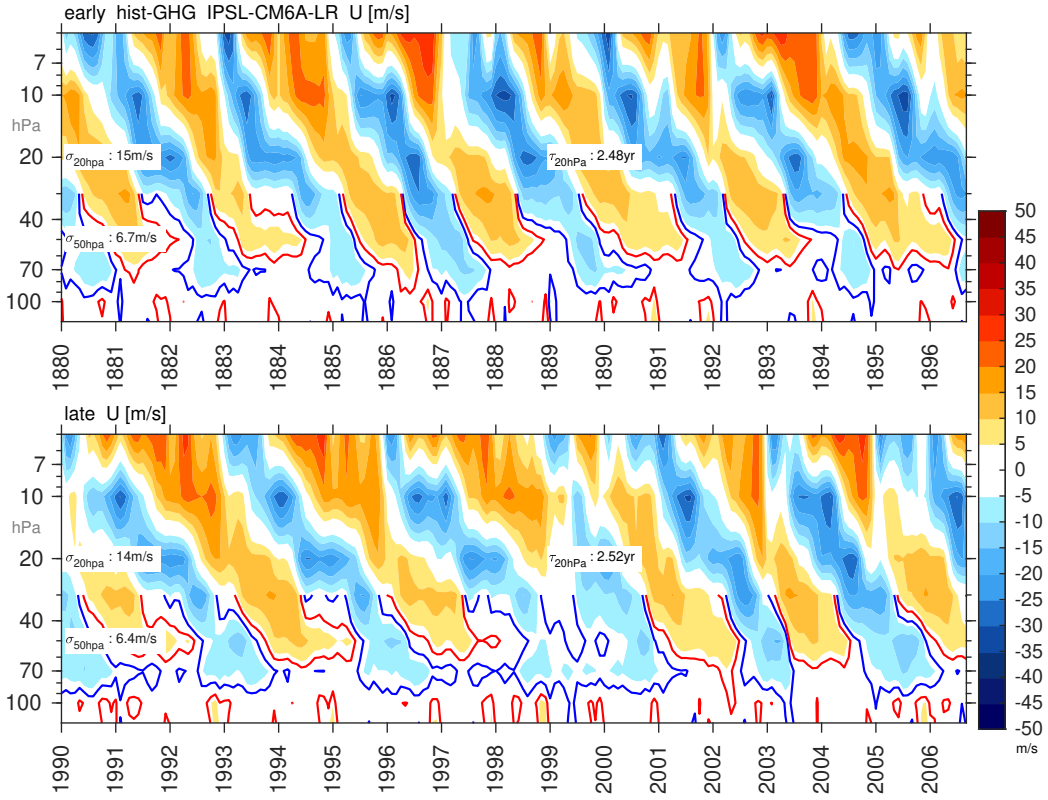

Figure S4. As in Figure S1 but for IPSL-CM6A-LR.

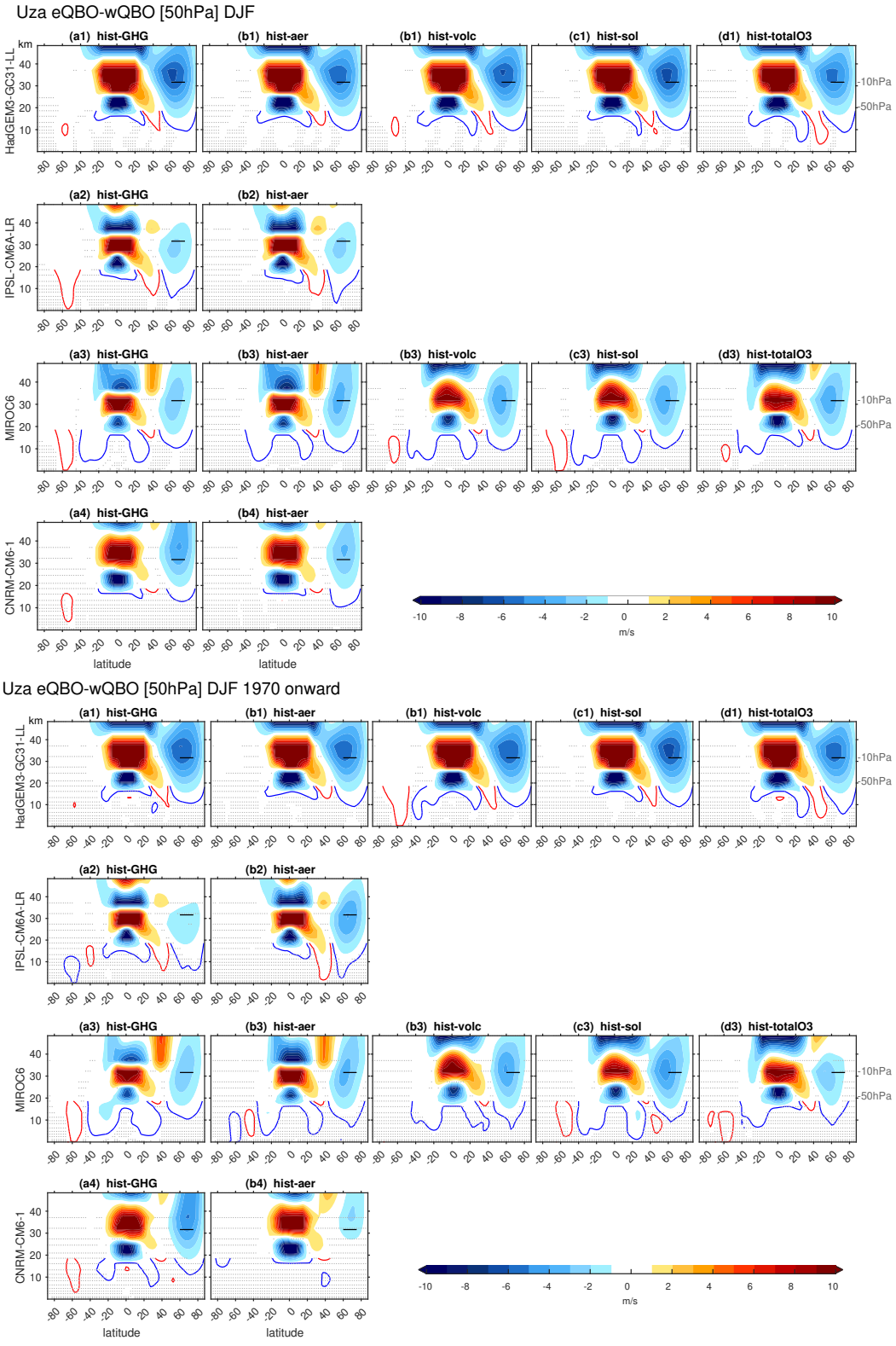

Figure S5. As in Figure 1 in the main text but for compositing instead of a regression approach. We also include the corresponding figure but for 1970 and onward only (high GHGs, high aerosols, and ozone depletion).

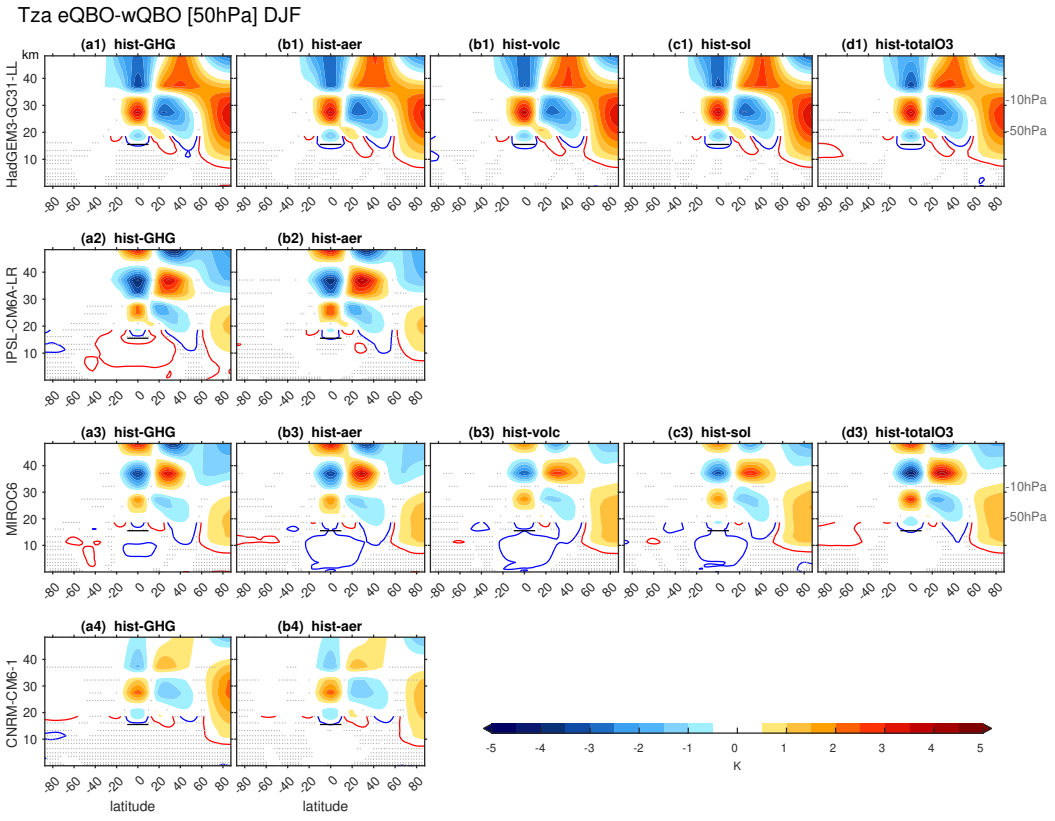

Figure S6. As in Figure 2 in the main text but for compositing instead of a regression approach.

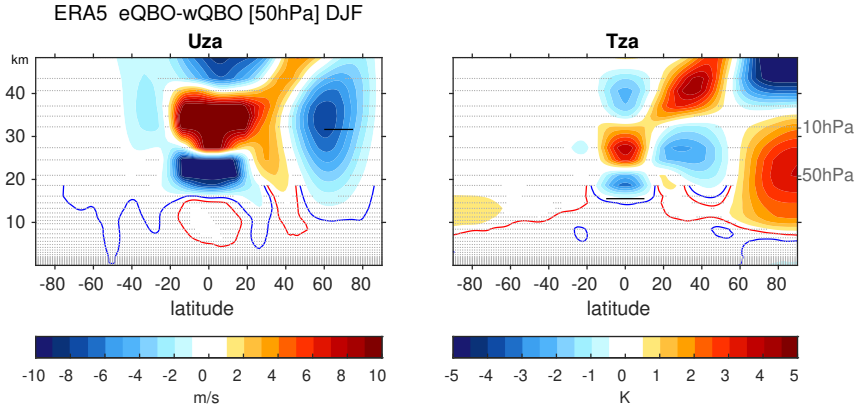

Figure S7. As in Figure 3 in the main text but for compositing instead of a regression approach.

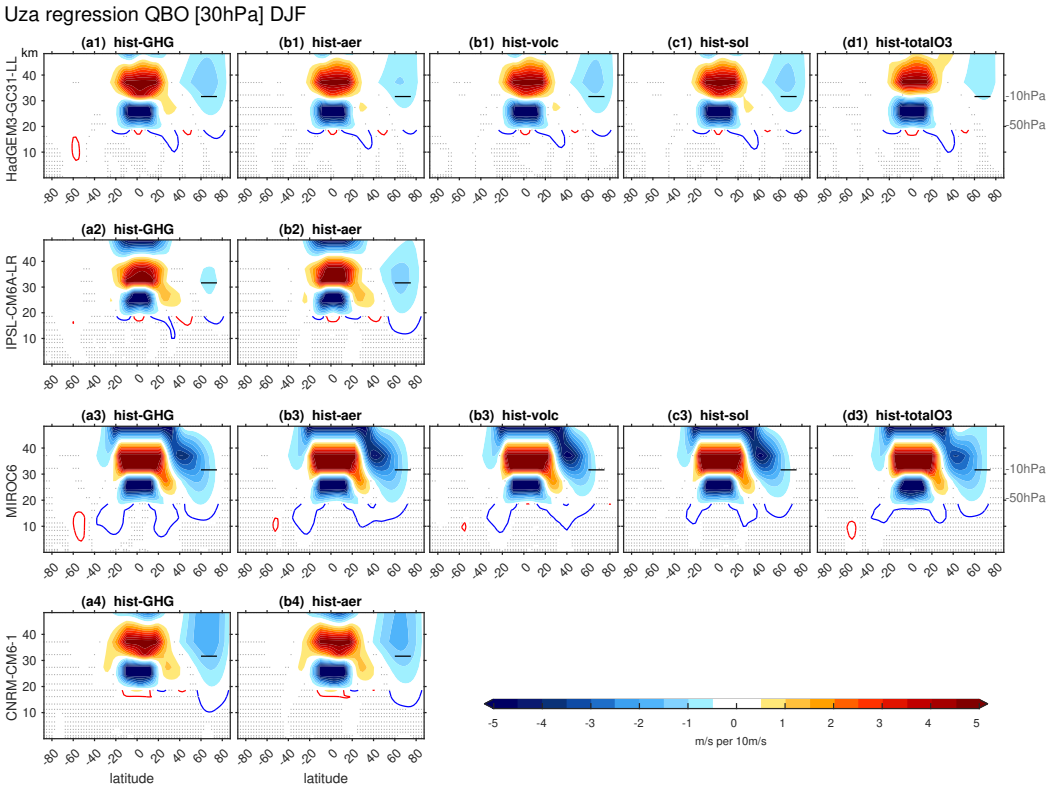

Figure S8. As in Figure 1 in the main text but for the QBO defined at 30hpa instead of 50hPa.

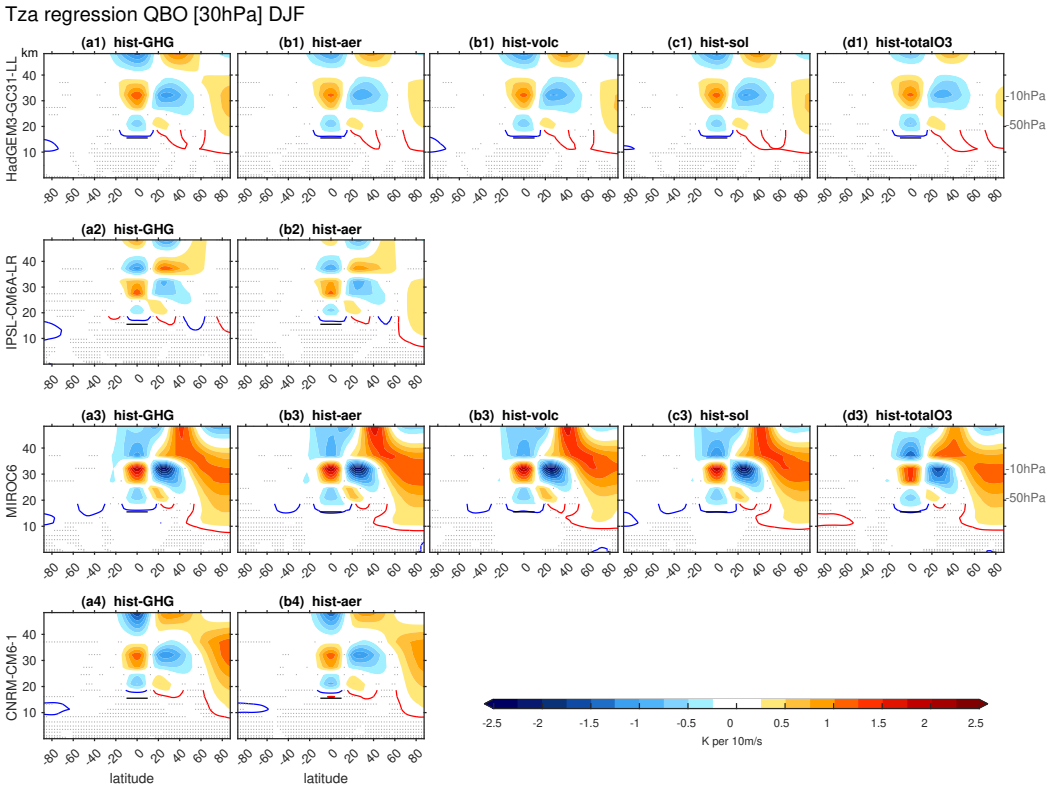

Figure S9. As in Figure 2 in the main text but for the QBO defined at 30hpa instead of 50hPa.

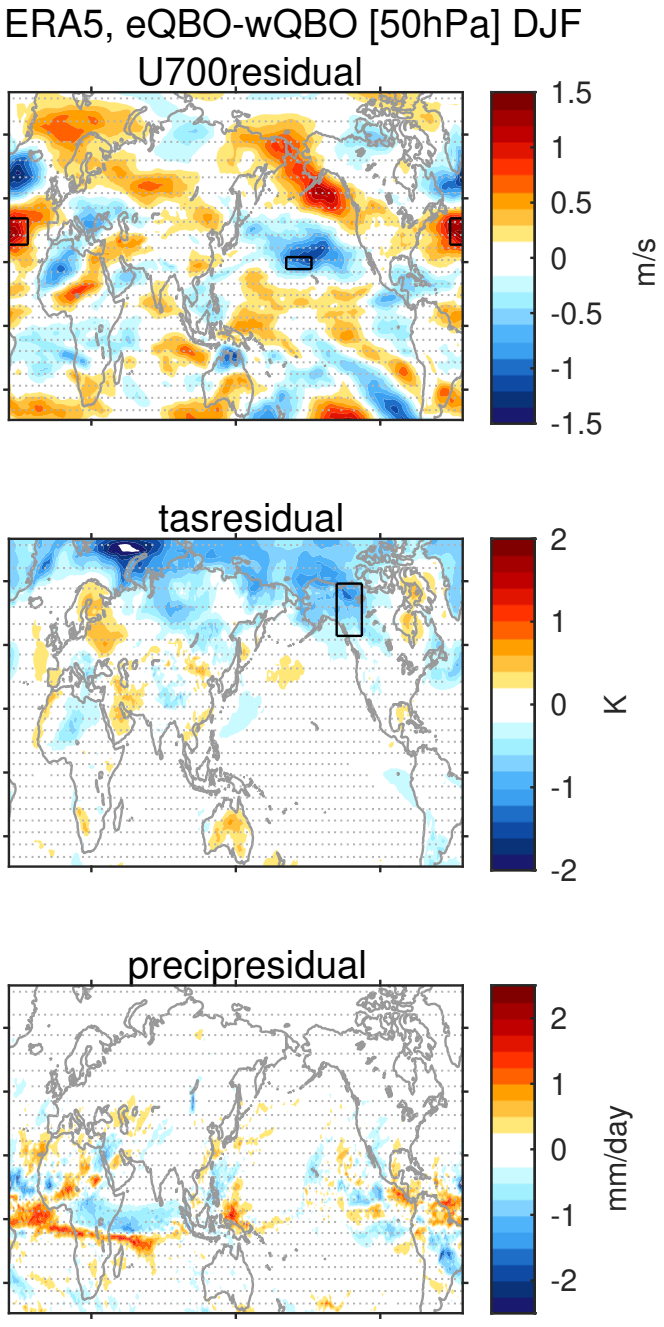

Figure S10. Temperature, U700, and precipitation responses to the QBO using ERA5 from 1957-2023 after using linear regression to exclude linear variability associated with the Nino3.4 index.

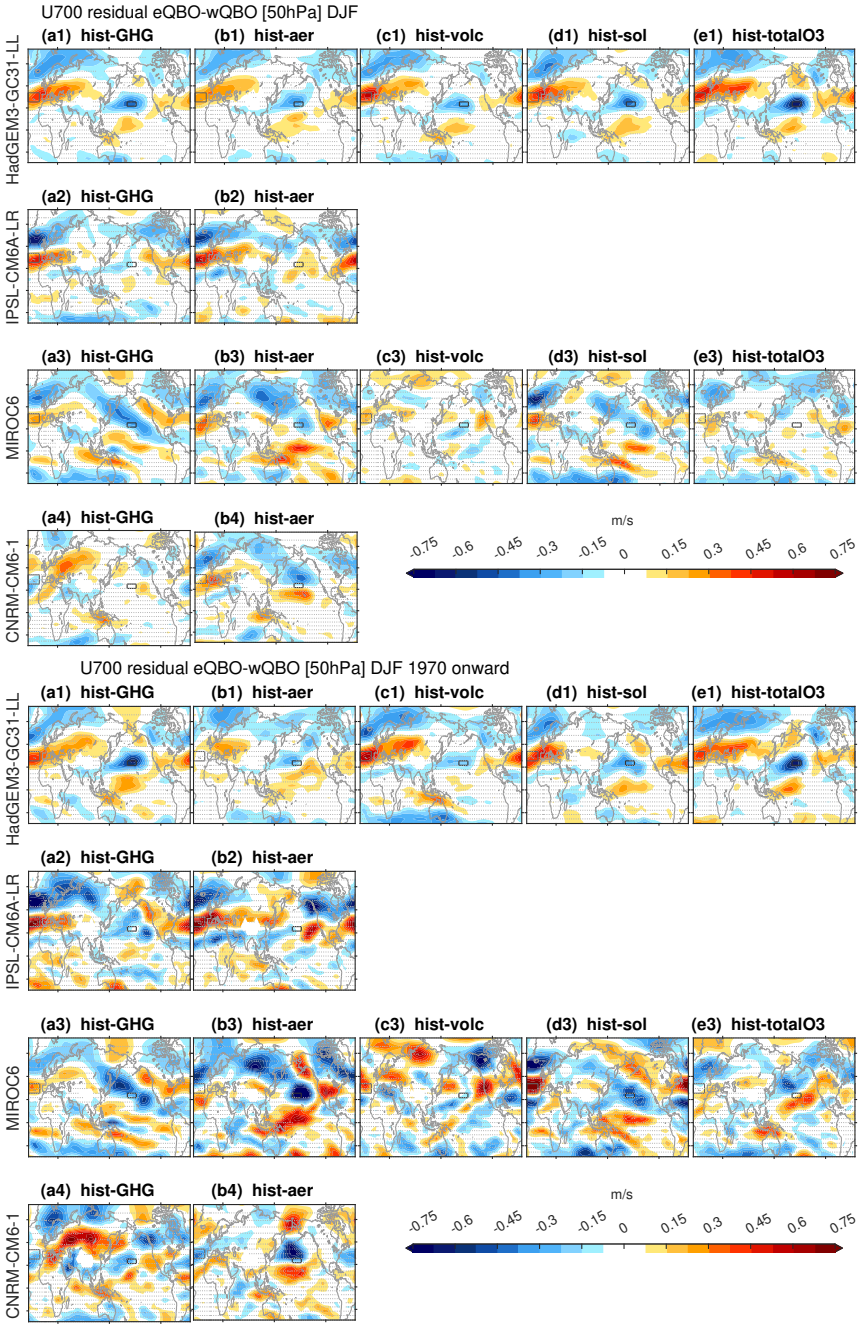

Figure S11. As in Figure 6 in the main text but after using linear regression to exclude linear variability associated with the Nino3.4 index both over the full period and also since 1970. The corresponding figure but for ERA5 from 1957 to 2023 is shown in Supplemental Figure S10.

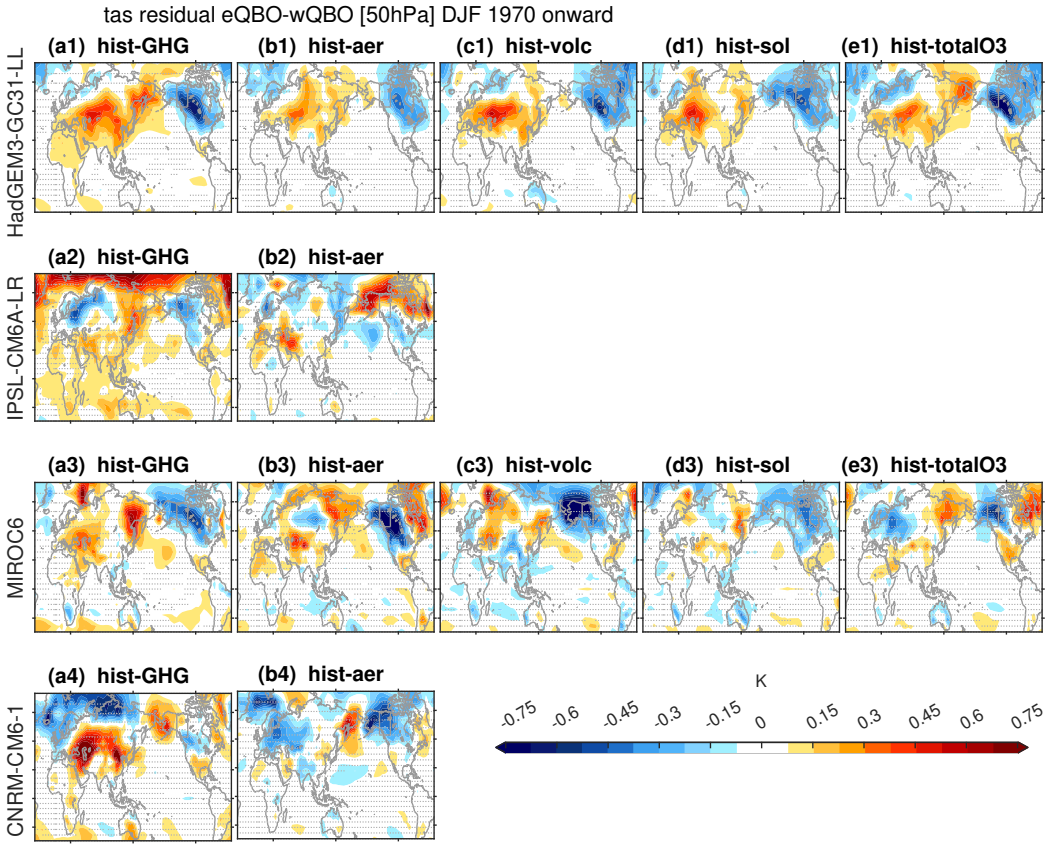

Figure S12. As in Figure 9 in the main text but for the period since 1970.

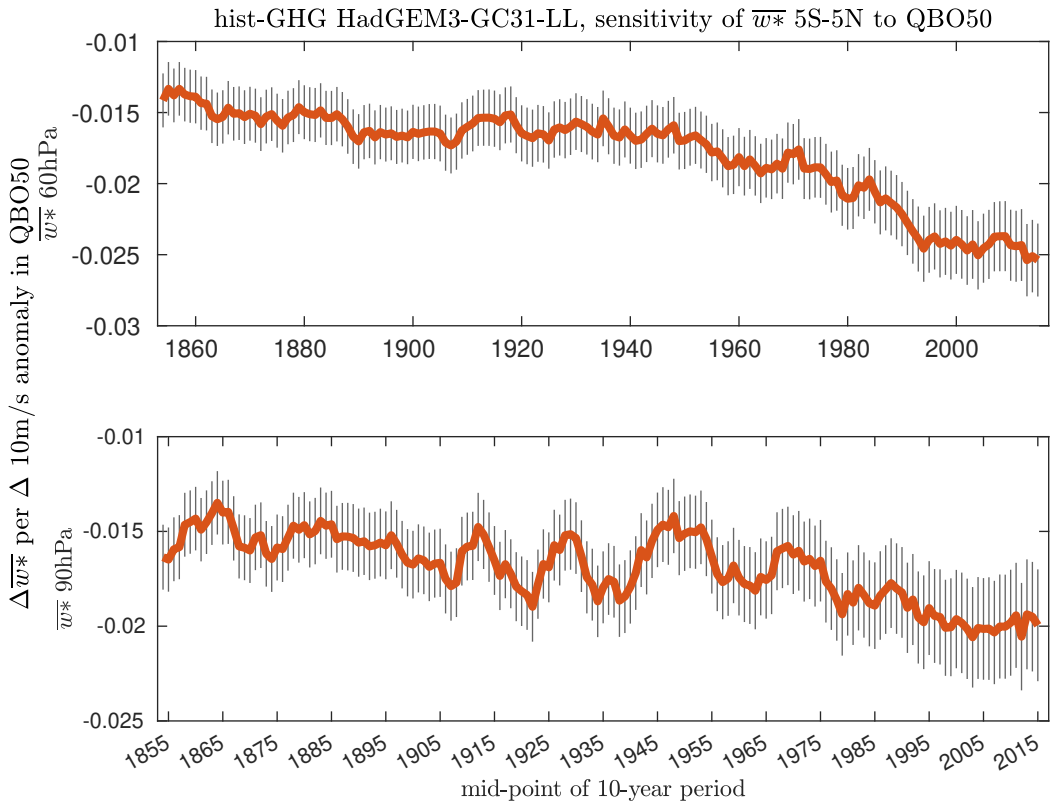

Figure S13. Regression coefficient of equatorial $\overline{w*}$ at 60hPa and at 90hPa per 10m/s change in QBO winds at 50hPa for rolling 10-year chunks of data in the hist-GHG experiment from HadGEM3. Note that the regression coefficient is always negative (i.e., eQBO leads to upwelling), but that the relationship intensifies in a warmed climate with higher GHGs as discussed in the main text. The 95% uncertainty bounds on the regression coefficient as given by a Student-t test is indicated with a vertical line. Units are mm/sec per 10m/s.